CHEMICAL ENGINEERING TRANSACTIONS
VOL. 54, 2016
A publication of AIDIC
The Italian Association of Chemical Engineering
Online at www.aidic.it/cet
Guest Editors: Selena Sironi, Laura Capelli

ISBN 978-88-95608-45-7; **ISSN** 2283-9216

Evaluation of Metal Oxides Sensors for the Monitoring of O_3 in Ambient Air at Ppb Level

Laurent Spinelle[a], Michel Gerboles[a], Manuel Aleixandre[b], Fausto Bonavitacola[c]

[a] European Commission, Joint Research Centre (JRC), Institute for Environment and Sustainability (IES), Ispra, Italy
[b] Grupo de I+D en Sensores de Gases, ITEFI, CSIC. Madrid, Spain
[c] Phoenix Sistemi & Automazione s.a.g.l., Muralto (TI), Switzerland
michel.gerboles@jrc.ec.europa.eu

Hereafter we present a laboratory evaluation of commercially available and prototype metal oxide sensors for the monitoring of O_3 in ambient air at ppb level. The tests includes the determination of the sensor response time, their calibration function, the evaluations of repeatability, short and long term drifts, the hysteresis effect and the matrix effect. Interferences from gaseous compounds, temperature and humidity parameters are also evaluated.

1. Introduction

Gas sensors are identified as emerging devices for indicative measurements as defined in the European Directive for Air Quality (2008/50/EC, 2008). Compared to reference measurements, gas sensors would allow air pollution monitoring at lower cost. Recent development in sensors platforms mainly focused on the use of amperometric sensors (Mead et al., 2013 and Castell et al., 2013) because of the high linearity of their response and their limited drift over time. Conversely, this type of sensors suffers from a lack of selectivity that makes especially difficult to distinguish between ozone (O_3) and nitrogen dioxide (NO_2) (Spinelle et al., 2014.). Their wide application is also limited by their relative high price and short life time. On the contrary, Metal Oxides sensors (MOx) can be easily manufactured resulting in a moderate price. Unfortunately, MOx sensors have been shown by experiment to be difficult to calibrate because of their lack of linearity and their dependence on interfering variables as for example temperature and humidity (Gerboles and Buzica, 2009). Moreover, the stability of their calibration function over long period (longer than 100 days) is also a limitation to their applicability in field studies (Spinelle et al., 2015). Conversely, MOx sensors appear to be enough sensitive for monitoring inorganic gases in ambient air (Aleixandre and Gerboles, 2012).
In this paper we present an accurate evaluation of MOx sensors including commercial sensors and laboratory prototypes for monitoring O_3 in ambient air at ppb level in order to give quantitative estimation of the effect of several parameters on sensor measurements. The list of sensors consisted of: O_3 Sens 3000 (Unitec – IT), NanoEnvi (Ingenieros Assessores - SP), MiCS 2610 and Oz-47 (SGX Sensotech - CH), SP-61 (FIS – JP) and a prototype of WO_3 sensor designed by IMN2P (FR).
Experiments were conducted in a laboratory exposure chamber and were designed to evaluate several metrological parameters: response time, sensitivity, repeatability, limit of detection, short term drift (over 3 days), long term drift (over more than 100 days), interference from gaseous compounds (NO_2, NO, CO, CO_2, NH_3), differences of sensor values when measuring mixtures diluted with indoor, outdoor or filtered air and the effect of change of temperature and humidity. Additionally, the presence of hysteresis in sensor responses when changing O_3 concentration levels, temperature or humidity was studied. The experimental design follows the Protocol of evaluation of low-cost gas sensors for air pollution (Spinelle et al., 2013). Precise set up of experiments and details of the data treatment are given in this protocol. A discussion of the experimental results allows advising which parameters needs attention, correction or control. An attempt of estimating the sensor measurement uncertainty from laboratory experiment is also carried out.

2. Experimental setup

2.1 Data Acquisition of sensor values

The MICS 2610, O_3 Sens 3000 and SP-61 were connected to a USB powered Data Acquisition boards (DAQ) from National Instrument (NI-USB 6343 and NI-USB 6210). Oz-47 sensors include their own integrated circuits (PCB) in charge of data acquisition, allowing direct connection using an in-house developed multi-serial to USB port. The prototype of WO_3 sensor of IMN2P was mounted on a "Metal Oxide Semiconductor Gas Sensor Evaluation Kit" (MiCS-EK1 - CH).

The sensors were not calibrated by the manufacturers except for the NanoEnvi and SENS 3000 sensors. The sensors, generally two sensors per brand model, were installed inside the JRC laboratory exposure chamber for evaluation. All sensor's electronic parts were covered with Teflon tape to avoid any chemical reaction near by the sensitive layer of the sensors before being inserted in the exposure chamber.

2.2 Exposure chamber

The exposure chamber is described elsewhere (Spinelle et al., 2014). It is able to generate gaseous mixtures and to control humidity, temperature and wind velocity. All parameters are automatically and independently measured, set and controlled. It can accommodate several sensors for simultaneous testing with an internal volume of about 120 l. Conversely to other exposure chambers, the reference values of all compounds are measured allowing the full traceability to national/international units when evaluating sensors.

Two MicroCal 5000 (MCZ Gmbh, DE) generators were used for generating O_3. These generators are equipped with UV lamps placed in Thermo insulted chamber whose UV beam is controlled by a regulated current intensity. The intensity of the current applied to the UV lamp and the total flow of zero air of the generator were controlled by the exposure chamber LabView software. Mixtures of gaseous interferents were generated with an in-house designed permeation system, using NH_3, NO_2, SO_2 and HNO_3 permeation tubes from KinTec (G) and Calibrage (F). CO mixtures were directly generated by dynamic dilution from highly concentrated cylinders of Air Liquide (F). Reference measurements methods were used for O_3 (Thermo Environment TEI 49C UV-photometer), NO/NOx/NO_2: (Thermo Environment 42 C chemiluminescence analyser), SO_2 (Environment SA AF 21 M fluorescent analyser), CO (Thermo Environment 48i-TLE NDIR analyser) and NH_3 (Thermo Environment Model 17i, courtesy of monitoring network of Bolzano/Bozen – IT). For CO_2, an infrared sensor, Gascard NG 0-1000 ppm (Edinburg Sensors – UK) was used. It was calibrated with a CO_2 cylinder (369 ppm, Air Liquide - F) and zero air obtained from a cylinder of ultra pure Nitrogen.

2.3 Protocol of evaluation of sensors

The evaluation of the sensor was carried out against the limit or target values (LV) defined in the Directive with corresponding averaging time of one hour. The full scale of the O_3 sensors were set to 110 ppb by observing the range of measured values at rural sites. The response time of sensors is evaluated as 90% of the final stable value, when concentration changes from 0 to 90 ppb. It is used to set the length of all tests of the protocol and to check if the sensor is able to reach stability within averaging time. Then, a pre-calibration of the sensor is performed at several concentration levels, at the average exposure conditions. The objective of this calibration is to eliminate any bias at the mean temperature and relative humidity and to establish a draft model equation if needed. Then repeatability, short and long term drifts of the sensors are determined. Hysteresis is evaluated by repeating the pre-calibration experiment in an increasing ramp, a decreasing ramp and an increasing ramp of test gas, in a row. The repeatability values impose limits on the accuracy of the calibration. The identification of significant interferences was performed one at time at constant O_3 levels with all influencing variables kept constant. Temperature and humidity were tested between 22 ±10 °C by step of 5 °C and between 60 ± 20% by step of 10% respectively. The sensor response was also tested using filtered air, indoor air and outdoor air. Gaseous interferences were tested at two levels: at zero level and at the expected average values observed in the selected micro-environment. For some sensors, also ambient pressure, power supply and wind velocity were tested. If a trend in the long term drift or significant hysteresis or interference effects are identified, they were accounted as uncertainty contributions.

3. Results

Figure 1 gives an example of calibration, long drift, temperature, humidity, matrix and hysteresis effect on the sensor response for the FIS SP-61.

3.1 Response time

The response time of sensors, t_{90}, was computed by estimating $t_{0\text{-}90}$, the time needed by the sensor to reach 90 ppb and $t_{90\text{-}0}$, the time needed to reach zero starting at 90 ppb. During tests, temperature, humidity and the possible interfering gas compounds were kept constant. Table 1 gives the response times of the sensors. They remained within half an hour with similar rise time and lag time.

3.2 Calibration

The calibration levels included 90, 40, 0, 60, 20, 110 ppb in randomized order to take into account any possible hysteresis effect. Generally, calibration lines were not found linear. In fact, a saturation phenomenon of the response of sensors was observed as already reported in literature (Lösch et al. 2008). Several models were fitted using a weighted Levenberg Marquardt non Linear Least square algorithm to address this saturation effect: Michelis Munten (Eq. 1), Hill equation (Eq. 2), exponential decay (Eq. 3), and simple polynoms of 2nd and 3rd order (Kurganov et al. 2001) where R is the sensor response at any O_3 level, R_{max} the maximum sensor response, $O_{3,Rmax/2}$ is the O_3 level at half of R_{max}, h is the slope at $O_{3,Rmax/2}$, C is the sensor response at 0, a is the response increase between C and Rmax and K is $1/O_{3,Rmax/2}$. Table 1 gives the standard uncertainty of lack of fit, the maximum and standard deviation of residuals computed using the experimental results. Within all fitted models, we selected the most appropriate using the smallest between:

- the uncertainty of lack of fit of the model (u(lof)), computed assuming a rectangular distribution for the maximum O_3 residual of the measuring function,
- and the minimum Akaike Information Criterion (Sakamoto et al. 1986), a proxy used to balance between the goodness of fit of the models and their complexity shown by the number of parameters to be estimated.

Table 1. Sensor's response time evaluate in exposure chamber (t_{90}, $t_{0\text{-}90}$ and $t_{90\text{-}0}$, after subtraction of the response time of the reference analyser). Calibration data are given for the best suited calibration function, with standard uncertainty of lack of fit u(lof), maximum (Max) residual and standard deviation (s) of residuals.

Sensors	t_{90}, min	$t_{0\text{-}90}$, min	$t_{90\text{-}0}$, min	Model	u(lof), ppb	Max residual, ppb	s residual, ppb
O_3 Sens 3000	52±36	39±29	65±39	Hill	2.0	2.0	1.1
NanoEnvi	9.8 ± 7.8	4.3 ± 3.3	15.3 ± 2.5	Hill	2.4	3.1	1.7
MiCS 2610	4.4 ± 8.1	1±1	9.9 ± 5.5	Decay	8.1	13.3	6.3
FIS SP-61	89 ± 111	115±153	63±39	Hill	2.9	4.2	2.2
WO_3 - IMN2P	8.8 ± 6.6	4.4 ± 3.2	13.1 ± 1.6	Hill	1.8	1.6	1.0

Using the AIC values, cubic calibration functions appears to be the most appropriate. However, the Hill equation models gave similar fitting with higher AICs values but lower standard uncertainty of lack of fit (u(lof)) and were preferred. The Hill equation being based on the maximum, minimum sensor response and the pollutant level corresponding to half of the maximum sensor response, they give better physical understanding of the calibration functions. For the MiCS sensors, an Exponential decay calibration function was selected as the use of a cubic model resulted in imaginary roots when the sensor values drifted out of the calibration range.

$$R = R_{max} O_3 / (O_{3,Rmax/2} + O_3) + C \quad (1)$$

$$R = R_{max} O_{3,Rmax/2}^h / \left(O_{3,Rmax/2} + O_3\right)^h + C \quad (2)$$

$$R = a(1 - e^{-KO_3}) + C \quad (3)$$

Table 2. Standard deviation at 0 and 100 ppb, limit of detections (lod) and repeatability at 100 ppb(r) for sensor minutes values. The four columns on the right gives the short term drift (Dss), its standard uncertainty u(Dss) and the long term drift trend (Dls) with its standard uncertainty u(Dls)

Sensors	sr (0/100 ppb)	lod, ppb	r at 100 ppb	Dss, ppb	u(Dss), ppb	Dls, ppb/days	u(Dls), ppb
O_3 Sens 3000	0.8/3.3	2.3	9.3	5.0	8.2	0.070±0.060	30.2
NanoEnvi	0.5/2.0	1.5	5.7	4.7	5.1	0.081±0.010	11.4
MiCS 2610	0.2/0.2	0.5	0.5	2.0	2.5	-0.009±0.016	19.4
FIS SP-61	-/19.8	-	56	12.9	15.1	-0.007±0.180	14.5
WO_3 - IMN2P	0.3/0.2	1.0	0.7	2.7	4.8	-0.019±0.145	29.2

3.3 Repeatability and limit of detection

The repeatability and the limit of detection of the sensors (see Table 2) were estimated by calculating the standard deviation of sensor values, sr, with the sensor measuring at 0 and at about 100 ppb while other exposure conditions were kept constant. The repeatability of sensor was computed as 2√2 sr (sr at 100 ppb) and the limit of detection was estimated as 3sr, (sr at 0 ppb).

3.4 Short term and long term drifts

For the short term drift, sensor responses were evaluated at 0, 60 and 90 ppb on 3 consecutive days, each of them being separated by a period of time between 12 and 36 hours. The mean deviations between days of the

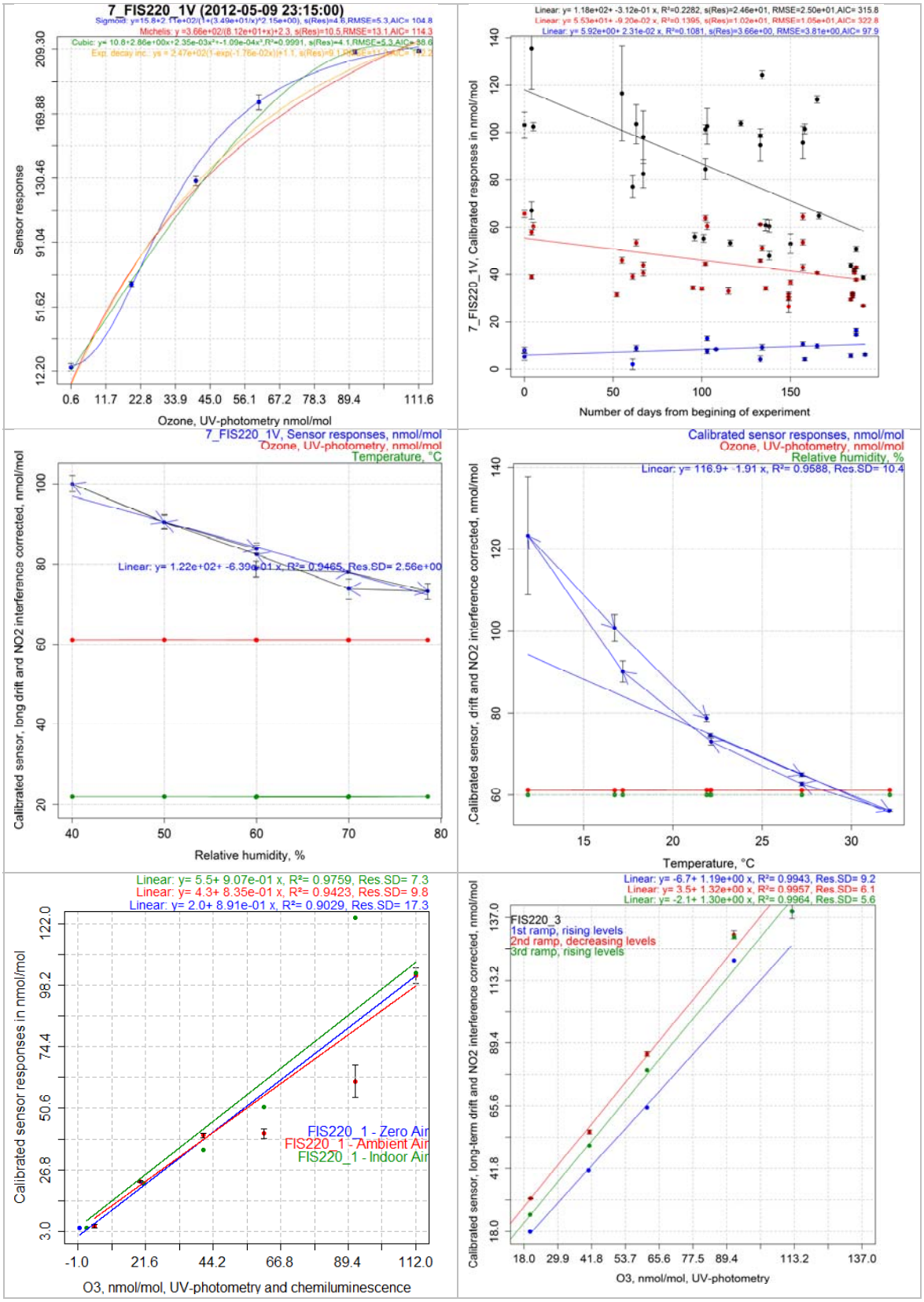

Figure 1: Example of estimation of the calibration function (top left), long term drift (top right), humidity (middle left) and temperature effect (middle right), matrix effect (bottom left) and effect of hysteresis of O_3 levels (bottom right).

sensor responses, Dss, were calculated. The contribution to the measurement uncertainty u(Dss) was calculated using a quadratic sum of Dss and a pooled standard deviation of the Dss at all concentration levels (Table 2).
For the long term drift, a similar approach was used measuring sensor responses during 6 months about once a week. The long term drift, Dls, was estimated using the trends of the sensor responses from the beginning to the end of all experiments (150 days). The standard uncertainty of the long term drift u(Dls) was estimated using the slope of the trend and the scattering of measurement around this trend (Table 2).

3.5 Temperature and humidity effects

Sensors are influenced by changes of temperature or relative humidity. Two series of tests were conducted independently, generating ramps of temperature and humidity in a hysteresis cycle while gaseous levels in the chamber were kept constant. The ranges of temperature changed between 12 and 32 ºC (by step of 5 ºC) and the range of humidity was kept between 40% and 80% (by step of 10%). The results of the tests are given in Table 3, including sensitivity coefficients of the sensors to temperature and humidity and the contribution of these parameters to the measurement uncertainty. The standard uncertainties include both the contribution from the sensitivity coefficients and hysteresis effect.

3.6 Gaseous interfering compounds and matrix effect

The effect of NO_2, NO, CO, CO_2 and NH_3 were evaluated at two levels. The influence of each interfering compound was determined separately. The tests were carried out at 22°C and 60 % of relative humidity and in absence of other interfering compounds. For each compound, we determined the sensitivity coefficient and the difference of sensor responses divided by the level of the interfering compound (see Table 3). The sensitivity coefficients were calculated changing NO_2 from 0 to 90 ppb, NO from 0 to 100 ppb, CO from 460 to 8230 ppb, NH_3 from 0 to 85 ppb and CO_2 from 0 to 390 ppm. Table 3 gives for each pollutant the uncertainty contribution calculated by multiplying the sensitivity coefficient with the standard uncertainty of each compound corresponding to the standard deviation of the distribution of the pollutants at rural sites (6.6 ppb for NO_2, 7.2 ppb for NO, 49 ppb for NH_3, 310 ppb for CO and 17.2 ppm for CO_2) (Spinelle et al., 2013). A linear correction was applied to the sensor values in order to correct for the long term drift before estimating the effect of gaseous interfering compounds.
The completeness of the gaseous interference testing was checked by evaluating the effect of air matrix on the sensor response. Three different air matrixes (filtered air, ambient air and indoor air) were used for dilution using the calibration levels. Three calibration lines were plotted, one for zero air, one for ambient air and one for indoor air and were compared. In general, all sensors showed negligible matrix effect since the calibration lines were similar. The difference of slope of the three lines ranged from to 1 % for the MICS 2610 and for the WO3-IMN2P, 6% for the FIS SP-61, 30 % for the NanoEnvi sensors and 35 % for the SENS 3000 (relative standard deviations RSD).

3.7 Hysteresis effect

The estimation of the dependence of sensors toward hysteresis was carried out using the calibration levels with a ramp of rising concentrations followed with a ramp of decreasing levels and finally with another rising ramp. Three calibration lines were plotted, one for each ramp. In general, the sensors showed very little hysteresis effect with only small changes of intercept values for linear lines. The relative standard deviation (RSD) of the slope of the three lines were found to be 1 % for the MICS 2610 and for the WO3-IMN2P, 6 % for the FIS SP-61, 10 % for the NanoEnvi sensors and 9 % for the SENS 3000.

Table 3. Gaseous interfering compounds: sensitivity coefficients (ppb/ppb or ppb/ppm for CO_2) ± standard uncertainty in ppb. For temperature and humidity: sensitivity coefficients (ppb/°C or ppb/%) / standard uncertainty in ppb.

Sensors	NO_2	NO	CO	CO_2	NH_3	Temperature	Humidity
O_3 Sens 3000	0.015/0.1	-0.061/0.4	$2.3\ 10^{-3}$/0.7	-0.076/1.3	$-1.1\ 10^{-3}$/0.1	-3.86/76	-0.65/12.3
NanoEnvi	0.014/0.1	$-1.9\ 10^{-3}$/0.1	$-7.9\ 10^{-4}$/0.2	$2.2\ 10^{-3}$/0.0	$8.0\ 10^{-4}$/0.0	-0.7/2.6	-0.02/2.6
MiCS 2610	0.081/0.5	-0.016/0.1	$-3.5\ 10^{-4}$/0.1	$1.9\ 10^{-3}$/0.1	$-1.0\ 10^{-3}$/0.1	-3.1/48	0.84/15.6
FIS SP-61	0.024/0.2	0.13/0.9	$9.9.10^{-4}$/0.3	$-1.2\ 10^{-2}$/0.3	$3.0\ 10^{-2}$/1.5	-2.3/37.8	-0.46/8.7
WO_3 - IMN2P	0.19/1.2	$-1.4\ 10^{-4}$/0.0	$3.6\ 10^{-5}$/0.0	$3.2\ 10^{-4}$/0.0	$3.1\ 10^{-4}$/0.2	-1.33/9.2	-0.35/6.7

4. Conclusions

This laboratory evaluation shows response time of 5 min for the MICS 2610 and 10 min for the WO3-IMN2P and NanoEnvi while the SENS 3000 and FIS SP-61 were much slower (t_{90} of 50 min and 90 min respectively). Additionally, the lag times were about 2 times faster than the rise with the exception of the FIS SP41. In

general, the calibration functions were fitted using sigmoidal models, the WO3-IMN2P sensor being the nearest to linear sensor. Even if the NanoEnvi and Unitec were calibrated by the manufacturer, this did not result in a linear sensor response. Using our laboratory calibration with sigmoidal model, the lack of fit of the model appear to be limited, only the MICS 2610 presented significant residuals and at long O_3 levels caused by the use of an exponential decay model.
The low scattering of sensor responses resulted in low limits of detection (a few ppb), high repeatability and limited short term drifts except for the FIS SP-61 that was found generally less precise than the other sensors. Conversely, the long term drift was shown to be a major shortcoming of MOx sensors with uncertainty contribution between 10 and 30 ppb over 150 days making re-calibration of the sensor obligatory. The experiments showed that generally O_3 sensors do not suffer from gaseous interference from NO_2, NO, CO, CO_2 and NH_3, Moreover, the matrix effect experiment showed that there is likely other unknown interfering compounds that affect the SENSE 3000 and NanoEnvi sensors since they showed biases according to the complementary gas used for dilution (either filtered, indoor or outdoor air). NanoEnvi uses an algorithm that allows the correction for temperature and humidity changes on sensor values. The other sensors clearly showed that they are sensitive to these parameters in particular to temperature with uncertainty contribution up to 75 ppb while the effect on humidity is more limited. Finally, the sensors showed little hysteresis effect on O_3 level cycles. The presented results are only valid for the version of sensors under tests in the conditions and at the time of the tests.

Acknowledgments

This study was carried out within the EMRP Joint Research Project ENV01 MACPoll. The EMRP is jointly funded by the EMRP participating countries within EURAMET and the European Union. The authors wish to acknowledge the collaboration of Unitec S.r.l.-IT, Ingenieros Assessores S.A.-SP, SGX Sensotech-CH, IMN2P Marseille University-FR, MIKES and the Aalto University-FR and of our colleague Friedrich Lagler.

Reference

Aleixandre M., Gerboles M., 2012, Review of Small Commercial Sensors for Indicative Monitoring of Ambient Gas. Chemical Engineering Transactions 30, 169–74. doi:10.3303/CET1230029.

Castell N., Viana M., Minguillón M. C., Guerreiro C. and Querol X., 2013, Real-World Application of New Sensor Technologies for Air Quality Monitoring, http://acm.eionet.europa.eu/docs/ETCACM_TP_2013_16_new_AQ_SensorTechn.pdf.

European Commission, 2008, Directive 2008/50/EC of the European Parliament and the Council of 21 May 2008 on Ambient Air Quality and Cleaner Air for Europe, Official Journal of the European Union, L152/1.

Gerboles M., Buzica D., 2009, Evaluation of Micro-Sensors to Monitor Ozone in Ambient Air. Joint Research Center for Environment and Sustainability, EUR 23676 EN, DOI 10.2788/5978.

Kurganov B.I., Lobanov A.V., Borisov I.A., Reshetilov A.N., 2001. Criterion for Hill equation validity for description of biosensor calibration curves. Analytica Chimica Acta, 427, 11–19.

Lösch M., Baumbach M., Schütze A., 2008. Ozone detection in the ppb-range with improved stability and reduced cross sensitivity. Sensors and Actuators B: Chemical, 130, 367–373.

Moré J.J., 1978, The Levenberg-Marquardt algorithm: implementation and theory, in Lecture Notes in Mathematics 630: Numerical Analysis, G.A. Watson (Ed.), Springer-Verlag: Berlin, pp. 105-116.

Mead M. I., Popoola O. A. M., Stewart G. B., Landshoff P., Calleja M., Hayes M., Baldovi J. J. , McLeod M.W., , Hodgson T.F., Dicks J., Lewis A., Cohen J., Baron R., Saffell J.R., Jones R. L., 2013, The use of electrochemical sensors for monitoring urban air quality in low-cost, high-density networks. Atmospheric Environment, 70, 186–203. http://doi.org/10.1016/j.atmosenv.2012.11.060

Sakamoto Y., Ishiguro M., Kitagawa G., 1986. Akaike Information Criterion Statistics. D. Reidel Publishing Company.

Spinelle L., Aleixandre M., Gerboles M., 2013, Protocol of evaluation and calibration of low-cost gas sensors for the monitoring of air pollution, EUR 26112. doi: 10.2788/9916, Publications Office of the European Union, http://publications.jrc.ec.europa.eu/repository/handle/JRC83791

Spinelle L., Aleixandre M., Gerboles M., 2014, Report of laboratory and in-situ validation of micro-sensor for monitoring ambient air - Ozone micro-sensors, αSense, model O3-B4, Reports No. EUR 26681. Publications Office of the European Union. http://publications.jrc.ec.europa.eu/repository/handle/JRC90463

Spinelle L., Gerboles M., Villani M. G., Aleixandre M., Bonavitacola F., 2015, Field calibration of a cluster of low-cost available sensors for air quality monitoring. Part A: Ozone and nitrogen dioxide. Sensors and Actuators B: Chemical, 215, 249–257. http://doi.org/10.1016/j.snb.2015.03.031